St. Petersburg Polytechnic University Journal. Physics and Mathematics. 2023. Vol. 16. No. 4
Научно-технические ведомости СПбГПУ. Физико-математические науки. 16 (4) 2023

BIOPHYSICS AND MEDICAL PHYSICS

Original article
DOI: https://doi.org/10.18721/JPM.16413

DETERMINING THE SIZE DISTRIBUTION FUNCTION OF IRREGULARLY SHAPED PARTICLES FOR HUMAN BLOOD CELLS AND FINDING THEIR ERYTHROCYTE PARAMETERS (*IN VIVO* CASE)

A. P. Golovitskii[1], *V. G. Kontsevaya*[2],[1]✉, *K. G. Kulikov*[1], *K. T. Koshlan*[3]

[1] Peter the Great St. Petersburg Polytechnic University, St. Petersburg, Russia;

[2] Pskov State University, Pskov, Russia;

[3] St. Petersburg State University, St. Petersburg, Russia

✉ nkoncevoi@mail.ru

Abstract. This article continues the authors' research aimed at constructing and developing a mathematical model used both to determine the size distribution function of human blood cells in vivo, and to find blood parameters used in medical practice. At this stage of the work, the nonsphericity of blood particles was taken into account and the convergence of processes describing multiple scattering of laser radiation by blood was optimized through the use of the method of extended boundary conditions, which made it possible to increase the possibilities of using the T-matrix method. The mathematical model for the analysis of biological processes has received material embodiment in a new software package. Regularization parameters are determined automatically based on specified kernel errors and "measured" data using different criteria. It is shown that, using the developed model, it is possible to theoretically predict the number of erythrocytes of abnormal size in a biomaterial based on measuring the width of the found erythrocyte size distribution.

Keywords: laser technologies, Tikhonov regularization, EBCM, erythrocyte index, unspherulated particle

Citation: Golovitskii A. P., Kontsevaya V. G., Kulikov K. G., Koshlan K. T., Determining the size distribution function of irregularly shaped particles for human blood cells and finding their erythrocyte parameters (in vivo case). St. Petersburg State Polytechnical University Journal. Physics and Mathematics. 16 (4) (2023) 160–180. DOI: https://doi.org/10.18721/JPM.16413

Научная статья
УДК 517.95+577.3+535.8+519.6
DOI: https://doi.org/10.18721/JPM.16413

НАХОЖДЕНИЕ ФУНКЦИИ РАСПРЕДЕЛЕНИЯ ЧАСТИЦ НЕРЕГУЛЯРНОЙ ФОРМЫ ПО РАЗМЕРАМ ДЛЯ КЛЕТОК ЧЕЛОВЕЧЕСКОЙ КРОВИ И ОПРЕДЕЛЕНИЕ ЕЕ ЭРИТРОЦИТАРНЫХ ПОКАЗАТЕЛЕЙ (*IN VIVO*)

А. П. Головицкий[1], *В. Г. Концевая*[2],[1]✉, *К. Г. Куликов*[1], *Т. В. Кошлан*[3]

[1] Санкт-Петербургский политехнический университет Петра Великого, Санкт-Петербург, Россия;

[2] Псковский государственный университет, г. Псков, Россия;

[3] Санкт-Петербургский государственный университет, Санкт-Петербург, Россия

✉ nkoncevoi@mail.ru

Аннотация. Данная статья продолжает исследования авторов, направленные на построение и развитие математической модели, используемой как для определения функции распределения клеток крови человека по размерам in vivo, так и для нахождения показателей крови, используемых в медицинской практике. На данном этапе работы была учтена несферичность частиц крови и оптимизирована сходимость процессов, описывающих многократное рассеяние лазерного излучения кровью за счет использования метода расширенных граничных условий, что позволило увеличить возможности применения Т-матричного метода. Математическая модель анализа биологических процессов получила материальное воплощение в новом программном комплексе. Параметры регуляризации определяются автоматически по заданным погрешностям ядра и «измеренным» данным с использованием разных критериев. Показана возможность, используя разработанную модель, теоретически предсказывать количество аномальных по размеру эритроцитов в биоматериале на основе измерения ширины найденного распределения эритроцитов по размерам.

Ключевые слова: лазерные технологии, многократное рассеяние, метод Т-матриц, метод регуляризации Тихонова, эритроцитарный индекс, несферулированная частица

Ссылка для цитирования: Головицкий А. П., Концевая В. Г., Куликов К. Г., Кошлан Т. В. Нахождение функции распределения частиц нерегулярной формы по размерам для клеток человеческой крови и нахождение ее эритроцитарных показателей (in vivo) // Научно-технические ведомости СПбГПУ. Физико-математические науки. 2023. Т. 16. № 4. С. 160–180. DOI: https://doi.org/10.18721/JPM.16413

Introduction

Hemorheological and microcirculatory dysfunctions of the human body accompany, as a rule, most diseases and complications. Since 99% of the total volume of blood corpuscles are red blood cells, the study of the functional characteristics of these cells is crucial. The characteristic sizes of erythrocytes, their refractive indices and mechanical properties, as well as the dynamics of changes in such indicators of the state of the body should undoubtedly be investigated in cases of various pathological conditions; such studies are always of major importance.

The human erythrocyte is an elastic cell that has a rather complex discoid shape in its normal mature state. Moreover, under various external influences, with conditions of various kinds, discocyte (mature normal form of erythrocyte) can undergo a transition to other forms, for example platycide, acanocide, etc. [1].

A range of studies (see, for example, [2-5]) have explored the possibilities of theoretical investigation of the optical characteristics of dielectric bodies of different shapes and structures.

The classical problem of scattering light radiation by irregularly shaped particles is solved by direct numerical methods, which make it possible to reduce this problem to solving a system of algebraic equations or to the method of variable separation. In the first case, either an integral equation is constructed, or the expansion of fields is introduced with respect to vector spherical harmonics, i.e., solutions of the Helmholtz wave equation with their subsequent "joining" on the surface of the scatterer.

In our opinion, it is worth listing some successful approximations that allow to obtain rather satisfactory results.

First, it is the Rayleigh–Gans–Debye method [6]. Secondly, it is acceptable to use methods of geometric optics, especially in cases where particles can be considered large enough relative to the wavelength of the incident radiation [7]. Thirdly, these are methods of anomalous diffraction [8, 9]. Further, iterative methods deserve special mention [10]. We should also consider the Wentzel–Kramers–Brillouin method as well as the eikonal approximation [11, 12] as the most well-known method of anomalous diffraction. The latter is, in fact, the implementation of the approximation of short waves or high energies. Another notable approach is the perturbation method [13], which is based on the decomposition of an unknown solution to the scattering problem with respect to a small parameter in the vicinity of the exact solution. When applied to nonspherical particles, this means that the solution is sought as small deviations from the solution, which are caused by small deviations of the shape from the ideal spherical one.

In our opinion, the most convenient and reliable approach to solving the problem of light scattering by bodies of arbitrary shape is the method of integral equations, called the method of extended boundary conditions [14, 15], since it provides an accurate solution to the scattering problem (unlike other methods) by a particle of arbitrary shape; although this solution has the form of infinite series, it is acceptable. The maximum number of expansion terms required to achieve acceptable accuracy depends on the size, shape and refractive index of the scatterer.

In this paper, we investigate some aspects of the problem of light scattering by dispersed elements (blood cells in our case), which are irregular in shape and located in a medium of non-trivial structure (here it is the skin, a multilayered structure).

The problem of modeling scattering by dispersed structures with irregular configuration is set.

The study involves considering light scattering by a dispersed system (blood corpuscles), where the shape of the inhomogeneities is irregular and their orientation is arbitrary. This takes into account the effects of multiple scattering of light incident on a layered medium (human skin).

Such consideration includes several stages.

At the first stage, the problem of light scattering in the system is solved.

At the second stage, the reflection coefficient of a plane wave from a layered surface with a wavy shape is studied (the case of reflection of a Gaussian beam is taken).

At the third and final stage, a search is carried out for the size distribution function of blood corpuscles (scatterers of irregular shape placed in a layered medium). It is important to take into account that the simulated system is assumed to be placed in a layered medium.

Light scattering by the jth individual particle of arbitrary shape (matrix formulation)

Let us start considering the problem with the assumption that only red blood cells are present in the simulated dispersed medium (blood). It is fairly appropriate and does not contradict the problem statement, since the proportion of other blood corpuscles is about 1% of the hematocrit.

In a number of studies, the erythrocyte is considered as a structurally homogeneous sphere [16, 17], which can be taken a first approximation. With a deeper analysis (microscopic level), it is more correct to consider the erythrocyte as a body of irregular shape.

To find the field scattered by an ensemble of particles with irregular shape, we use the T-matrix method. It is rapid compared with most other methods of light diffraction theory based on a rigorous solution of Maxwell′s equations.

A dispersed inhomogeneous medium is considered in a three-dimensional coordinate system, and a linearly polarized plane wave falls on an ensemble of inhomogeneities. It is assumed that the wavelength is smaller than the typical size of red blood cells, that the surface of the dispersed scatterer is regular everywhere, so a continuous normal can be determined for it; Green′s theorem also holds true.

We write a system of Maxwell's equations for the electromagnetic field in the vicinity of a particle with the conditional number j_0, distorted by the presence of other particles:

$$\nabla \times \mathbf{H} = -ik\varepsilon\mathbf{E},\ \nabla \times \mathbf{E} = ik\mu\mathbf{H},\ \nabla \cdot \mathbf{E} = 0,\ \nabla \cdot \mathbf{H} = 0,$$

where k is the wavenumber; ε, μ are the dielectric and magnetic permeabilities of the medium.

At the boundary between the particle with the conditional number j_0 and the medium surrounding it, we require for the following boundary conditions to be satisfied:

$$\mathbf{n} \times \mathbf{E}_i - \mathbf{n} \times \mathbf{E}_s = \mathbf{n} \times \mathbf{E}_I,\ \mathbf{n} \times \mathbf{H}_i - \mathbf{n} \times \mathbf{H}_s = \mathbf{n} \times \mathbf{H}_I, \tag{1}$$

where $\mathbf{E}_i$, $\mathbf{E}_s$, $\mathbf{E}_I$ are the internal, scattered and incident fields, respectively.

The total field can be represented as

$$\mathbf{E}(r') = \mathbf{E}_I(r') + \mathbf{E}_s(r').$$

Let us write corresponding integral equation of the following form [18]:

$$\mathbf{E}_I(r') + \nabla \times \int_S \mathbf{n} \times \mathbf{E}(r) G(r, r')\,\mathrm{ds} + \frac{i}{k\varepsilon} \nabla \times \nabla \times \int_S \mathbf{n} \times \mathbf{H}(\mathrm{r}) \times G(r, r')\,\mathrm{ds} = 0. \tag{2}$$

The Green function in Eq. (2) is defined as follows [18]:

$$G(r, r') = \frac{ik}{\pi} \sum_{n=1}^{\infty} \sum_{m=-n}^{n} (-1)^m E_{mn} [\mathbf{M}^3_{-mn}(kr, \theta, \varphi) \cdot \mathbf{M}^1_{mn}(kr', \theta', \varphi') + \mathbf{N}^3_{-mn}(kr, \theta, \varphi) \cdot \mathbf{N}^1_{mn}(kr', \theta', \varphi')] \tag{3}$$

(for the case $r > r'$),

$$G(r, r') = \frac{ik}{\pi} \sum_{n=1}^{\infty} \sum_{m=-n}^{n} (-1)^m E_{mn} [\mathbf{M}^1_{-mn}(kr, \theta, \varphi) \cdot \mathbf{M}^3_{mn}(kr', \theta', \varphi') + \mathbf{N}^1_{-mn}(kr, \theta, \varphi) \cdot \mathbf{N}^3_{mn}(kr', \theta', \varphi')] \tag{4}$$

(for the case $r' > r$),
where $\mathbf{M}_{mn}$, $\mathbf{N}_{mn}$, $\mathbf{M}_{-mn}$, $\mathbf{N}_{-mn}$ are vector spherical harmonics.

Note that the choice of vector spherical harmonics should be made based on the invariance property (in the sense of closure), namely, that upon rotation of the coordinate system, such harmonics $\mathbf{M}_{mn}$, $\mathbf{N}_{mn}$ should be transformed independently of each other.

The following vector spherical harmonics satisfy the required invariance properties [18]:

$$\mathbf{M}^J_{mn}(rk) = (-1)^m d_n z^J_n(kr) \mathbf{C}_{mn}(\theta) \exp(im\varphi), \tag{5}$$

$$\mathbf{N}^J_{mn}(rk) = (-1)^m d_n \left[\frac{n(n+1)}{kr} z^J_n(kr) \mathbf{P}_{mn}(\theta) + \frac{1}{kr} \mathrm{z}^J_n \mathbf{B}_{mn}(\theta)\right] \exp(im\varphi), \tag{6}$$

$$\mathbf{B}_{mn}(\theta) = \mathbf{i}_\theta \frac{d}{d\theta} d^n_{om}(\theta) + \mathbf{i}_\varphi \frac{im}{\sin(\theta)} d^n_{om}(\theta), \tag{7}$$

$$\mathbf{C}_{mn}(\theta) = \mathbf{i}_\theta \frac{im}{\sin(\theta)} d^n_{om}(\theta) - \mathbf{i}_\varphi \frac{d}{d\theta} d^n_{om}(\theta), \tag{8}$$

$$\mathbf{P}_{mn}(\theta) = \mathbf{i}_r d^n_{om}(\theta),\ d_n = \sqrt{\frac{(2n+1)}{4n(\mathrm{n}+1)}}. \tag{9}$$

Any of the four spherical harmonics of the following form can be selected as a z_n^j function

$$j_n(z)=\sqrt{\frac{\pi}{2z}}J_{n+\frac{1}{2}}(z),\ y_n(z)=\sqrt{\frac{\pi}{2z}}Y_{n+\frac{1}{2}}(z),\ h_z^{(1)}=j_n(z)+iy_n(z),\ h_z^{(2)}=j_n(z)-iy_n(z),$$

$$d_{om}^n(\theta)=\frac{(-1)^{n-m}}{2^n n!}[\frac{(n+m)!}{(n-m)!}]^{1/2}(1-\cos^2(\theta))^{-m/2}\frac{d^{n-m}}{d\cos(\theta)^{n-m}}[1-\cos^2(\theta)^n].$$

Let us write the decomposition of the incident wave $\mathbf{E}_I$ on the surface of the jth particle with respect to vector spherical harmonics:

$$\mathbf{E}_I(j)=-\sum_{n=1}^{\infty}\sum_{m=-n}^{n}iE_{mn}[p_{mn}^j\mathbf{N}_{mn}^1+q_{mn}^j\mathbf{M}_{mn}^1]. \tag{10}$$

Similarly, we can write the decomposition with respect to vector spherical harmonics for both the internal field of the jth particle $E_i(j)$ and the scattered field $E_s(j)$:

$$\mathbf{E}_i(j)=-\sum_{n=1}^{\infty}\sum_{m=-n}^{n}iE_{mn}[d_{mn}^j\mathbf{N}_{mn}^1+c_{mn}^j\mathbf{M}_{mn}^1], \tag{11}$$

$$\mathbf{E}_s(j)=\sum_{n=1}^{\infty}\sum_{m=-n}^{n}iE_{mn}[a_{mn}^j\mathbf{N}_{mn}^3+b_{mn}^j\mathbf{M}_{mn}^3]. \tag{12}$$

In accordance with the procedures described in monograph [18], we sequentially substitute expressions (10), (11), (12), taking into account Green's functions (3), (4) and boundary conditions of the form (1), into the integral equation (2); then we obtain:

$$\frac{ik^2}{\pi}\int_s\sum_{n=1}^{\infty}\sum_{m=-n}^{n}(-1)^m[c_{mn}^j\mathbf{n}\times\mathbf{M}_{m'n'}^1+d_{mn}^j\mathbf{n}\times\mathbf{N}_{m'n'}^1]\begin{pmatrix}\mathbf{N}_{-mn}^3\\ \mathbf{M}_{-mn}^3\end{pmatrix}ds+$$

$$+\frac{ik^2}{\pi}\sqrt{\frac{\varepsilon_1}{\mu_1}}\int_s\sum_{n=1}^{\infty}\sum_{m=-n}^{n}(-1)^m[c_{mn}^j\mathbf{n}\times\mathbf{N}_{m'n'}^1+d_{mn}^j\mathbf{n}\times\mathbf{M}_{m'n'}^1]\begin{pmatrix}\mathbf{M}_{-mn}^3\\ \mathbf{N}_{-mn}^3\end{pmatrix}ds=-\begin{pmatrix}p_{mn}^j\\ q_{mn}^j\end{pmatrix}.$$

This expression can be rewritten in matrix form as

$$\begin{pmatrix}I_1^{21}+\tilde{m}\cdot I_1^{12} & I_1^{22}+\tilde{m}\cdot I_1^{11}\\ I_1^{22}+\tilde{m}\cdot I_1^{11} & I_1^{12}+\tilde{m}\cdot I_1^{21}\end{pmatrix}\begin{pmatrix}d^j\\ c^j\end{pmatrix}=-i\begin{pmatrix}p^j\\ q^j\end{pmatrix}, \tag{13}$$

where $\tilde{m}$ is the relative refractive index of the particle.

Furthermore,

$$\frac{ik^2}{\pi}\int_s\sum_{n=1}^{\infty}\sum_{m=-n}^{n}(-1)^m[c_{mn}^j\mathbf{n}\times\mathbf{M}_{m'n'}^1+d_{mn}^j\mathbf{n}\times\mathbf{N}_{m'n'}^1]\begin{pmatrix}\mathbf{N}_{-mn}^1\\ \mathbf{M}_{-mn}^1\end{pmatrix}ds+$$

$$+\frac{ik^2}{\pi}\sqrt{\frac{\varepsilon_1}{\mu_1}}\int_s\sum_{n=1}^{\infty}\sum_{m=-n}^{n}(-1)^m[c_{mn}^j\mathbf{n}\times\mathbf{N}_{m'n'}^1+d_{mn}^j\mathbf{n}\times\mathbf{M}_{m'n'}^1]\begin{pmatrix}\mathbf{M}_{-mn}^1\\ \mathbf{N}_{-mn}^1\end{pmatrix}ds=-\begin{pmatrix}a_{mn}^j\\ b_{mn}^j\end{pmatrix}.$$

This expression is written in matrix form as

$$\begin{pmatrix}a^j\\ b^j\end{pmatrix}=-i\begin{pmatrix}I_1'^{21}+\tilde{m}\cdot I_1'^{12} & I_1'^{22}+\tilde{m}\cdot I_1'^{11}\\ I_1'^{22}+\tilde{m}\cdot I_1'^{11} & I_1'^{12}+\tilde{m}\cdot I_1'^{21}\end{pmatrix}\begin{pmatrix}d^j\\ c^j\end{pmatrix}. \tag{14}$$

Combining expressions (13) and (14) produces the following equation

$$\begin{pmatrix} a^j \\ b^j \end{pmatrix} = -\begin{pmatrix} I_1'^{21} + \tilde{m} \cdot I_1'^{12} & I_1'^{22} + \tilde{m} \cdot I_1'^{11} \\ I_1'^{22} + \tilde{m} \cdot I_1'^{11} & I_1'^{12} + \tilde{m} \cdot I_1'^{21} \end{pmatrix} \begin{pmatrix} I_1^{21} + \tilde{m} \cdot I_1^{12} & I_1^{22} + \tilde{m} \cdot I_1^{11} \\ I_1^{22} + \tilde{m} \cdot I_1'^{11} & I_1^{12} + \tilde{m} \cdot I_1^{21} \end{pmatrix}^{-1} \begin{pmatrix} p^j \\ q^j \end{pmatrix}. \quad (15)$$

We introduce notations for matrices Q_{01}^{11}, Q_{01}^{31} and rewrite expression (15) in a more compact form:

$$\begin{pmatrix} a^j \\ b^j \end{pmatrix} = T_1^j \begin{pmatrix} p^j \\ q^j \end{pmatrix}, \; T_1^j = -Q_{01}^{11}(k, k_1) \cdot [Q_{01}^{31}(k, k_1)]^{-1}, \quad (16)$$

where the elements of matrix T_1^j are expressed as surface integrals.

Consider the normal $\mathbf{n} = n_x\mathbf{i} + n_y\mathbf{j} + n_z\mathbf{k}$.

For a body positioned arbitrarily, we obtain the following expression:

$$\mathbf{n}dS = \frac{\partial(y,z)}{\partial(\theta,\varphi)}\mathbf{i} + \frac{\partial(z,x)}{\partial(\theta,\varphi)}\mathbf{j} + \frac{\partial(\mathrm{x},y)}{\partial(\theta,\varphi)}\mathbf{k},$$

where the components of the vector follow the expressions

$$\begin{aligned} n_x dS &= [r(\theta,\varphi)r(\theta,\varphi)'_\varphi \sin(\varphi) + r(\theta,\varphi)^2 \sin^2(\theta)\cos(\varphi)]d\theta d\varphi - \\ &- r(\theta,\varphi)r(\theta,\varphi)'_\theta \sin^2(\theta)\cos(\varphi)d\theta d\varphi, \\ n_y dS &= [-r(\theta,\varphi)r(\theta,\varphi)'_\varphi \cos(\varphi) + r(\theta,\varphi)^2 \sin^2(\theta)\sin(\varphi)]d\theta d\varphi - \\ &- r(\theta,\varphi)r(\theta,\varphi)'_\theta \sin^2(\theta)\sin(\varphi)d\theta d\varphi, \\ n_z dS &= [r(\theta,\varphi)^2 \sin^2(\theta)\sin(\theta)\cos(\theta) - r(\theta,\varphi)r(\theta,\varphi)'_\theta \sin^2(\theta)]d\theta d\varphi. \end{aligned}$$

The equation of the particle surface in a spherical coordinate system takes the following form:

$$r(\theta,\varphi) = [\sin^2\theta(\frac{\cos^2\varphi}{a^2} + \frac{\sin^2\varphi}{b^2}) + \frac{\cos^2\theta}{c^2}]^{-1/2}. \quad (17)$$

Let us clarify the form of the equation for the ellipsoid of revolution:

$$r(\theta) = [\frac{\sin^2\theta}{a^2} + \frac{\cos^2\theta}{c^2}]^{-1/2} = \frac{ac}{\sqrt{a^2\cos^2\theta + c^2\sin^2\theta}}. \quad (18)$$

Note that a spheroid (ellipsoid of revolution) is obtained by rotating an ellipse around the semi-minor axis (oblate ellipsoid) or a major axis (prolate ellipsoid). Two of the three semi-axes of this ellipsoid have the same length. The aspect ratio of a spheroid is defined as the ratio of the semi-major axis *a* to the semi-minor axis *c* and describes the shape of a particle that varies from a sphere ($a/c = 1$) to a disk for an oblate ellipsoid or a needle for a prolate ellipsoid ($a/c \neq 1$).

For example, the ratio *a*/*c* determines an oblate spheroid, and c/a determines a prolate one. In this case, *a* is the length of the semi-axis along the *x* and *y* axes, and *c is* the length of the semi-axes along the *z* axis, which is the axis of rotation.

Using the formulas for the conversion between Cartesian and spherical coordinates, we obtain the following expressions:

$$\begin{aligned} n_r dS &= [\sin(\theta)\cos(\varphi)n_x + \sin(\theta)\sin(\varphi)n_y + \cos(\theta)n_z]d\theta d\varphi = r(\theta,\varphi)^2 \sin(\theta)d\theta d\varphi, \\ n_\theta dS &= [\cos(\theta)\cos(\varphi)n_x + \cos(\theta)\sin(\varphi)n_y - \sin(\theta)n_z]d\theta d\varphi = -r(\theta,\varphi)r(\theta,\varphi)'_\theta \sin(\theta)d\theta d\varphi, \\ n_\varphi dS &= [-\sin(\varphi)n_x + \cos(\varphi)n_y]d\theta d\varphi = -r(\theta,\varphi)r(\theta,\varphi)'_\theta d\theta d\varphi. \end{aligned}$$

Next, we substitute expressions for $\mathbf{n}dS$, $\mathbf{N}^1_{mn}$, $\mathbf{M}^1_{mn}$, $\mathbf{N}^3_{mn}$, $\mathbf{M}^3_{mn}$ into the surface integrals and obtain explicit expressions for them:

$$I^{11}_{mnmn} = (-1)^{(m+m')}\int_0^{\pi} i[md^n_{om}(\theta)b^{n'}_{om}(\theta) + m'd^n_{om}(\theta)b^{n'}_{om'}(\theta)]\cdot[\int_0^{2\pi} c_{mnmn}(\theta,\varphi)d\varphi]d\theta, \tag{19}$$

$$\begin{aligned} I^{12}_{mnm'n'} &= (-1)^{(m+m')}\int_0^{\pi} -[b^{n'}_{om}(\theta)b^{n'}_{om'}(\theta)\sin(\theta) + mm'd^n_{om}(\theta)d^{n'}_{om'}(\theta)/\sin(\theta)]\times \\ &\times[\int_0^{2\pi} c^2_{mnm'n'}(\theta,\varphi)d\varphi] - \frac{n(n+1)}{x}d^n_{om}(\theta)b^{n'}_{om'}(\theta)\sin(\theta)[\int_0^{2\pi} c^3_{mnm'n'}(\theta,\varphi)d\varphi] - \\ &-i\frac{n'(n'+1)}{x_1}d^n_{om}(\theta)d^{n'}_{om'}(\theta)\sin(\theta)[\int_0^{2\pi} c^4_{mnm'n'}(\theta,\varphi)d\varphi]d\theta, \end{aligned} \tag{20}$$

$$\begin{aligned} I^{21}_{mnm'n'} &= (-1)^{(m+m')}\int_0^{\pi} \frac{n'(n'+1)}{x_1}b^n_{om}(\theta)d^{n'}_{om'}(\theta)\sin(\theta)[\int_0^{2\pi} c^3_{mnm'n'}(\theta,\varphi)d\varphi] - \\ &-im\frac{n'(n'+1)}{x_1}d^n_{om}(\theta)d^{n'}_{om'}(\theta)/\sin(\theta)[\int_0^{2\pi} c^4_{mnm'n'}(\theta,\varphi)d\varphi] + \\ &+mm'd^n_{om}(\theta)d^{n'}_{om'}(\theta)/\sin(\theta) + \\ &+b^{n'}_{om}(\theta)b^{n'}_{om'}(\theta)\sin(\theta)[\int_0^{2\pi} c^5_{mnm'n'}(\theta,\varphi)d\varphi]d\theta, \end{aligned} \tag{21}$$

$$\begin{aligned} I^{22}_{mnm'n'} &= (-1)^{(m+m')}\int_0^{\pi} i[md^n_{om}(\theta)b^{n'}_{om'}(\theta) + m'd^{n'}_{om'}(\theta)b^n_{om}(\theta)]\cdot[\int_0^{2\pi} c^6_{mnm'n'}(\theta,\varphi)d\varphi] + \\ &+\frac{n'(n'+1)}{x_1}b^n_{om}(\theta)d^{n'}_{om'}(\theta)[\int_0^{2\pi} c^7_{mnm'n'}(\theta,\varphi)d\varphi] - \frac{n(n+1)}{x}d^n_{om}(\theta)b^{n'}_{om'}(\theta)\times \\ &\times[\int_0^{2\pi} c^8_{mnm'n'}(\theta,\varphi)d\varphi] + im\frac{n'(n'+1)}{x_1}d^n_{om}(\theta)d^{n'}_{om'}(\theta)[\int_0^{2\pi} c^9_{mnm'n'}(\theta,\varphi)d\varphi] + \\ &+im'\frac{n(n+1)}{x}d^n_{om}(\theta)d^{n'}_{om'}(\theta)[\int_0^{2\pi} c^{10}_{mnm'n'}(\theta,\varphi)d\varphi]d\theta, \end{aligned} \tag{22}$$

$$I'^{11}_{mnm'n'} = (-1)^{(m+m')}\int_0^{\pi} i[md^n_{om}(\theta)b^{n'}_{om}(\theta) + m'd^n_{om}(\theta)b^{n'}_{om'}(\theta)]\cdot[\int_0^{2\pi} f^1_{mnm'n'}(\theta,\varphi)d\varphi]d\theta, \tag{23}$$

$$\begin{aligned} I'^{12}_{mnm'n'} &= (-1)^{(m+m')}\int_0^{\pi} -[b^n_{om}(\theta)b^{n'}_{om'}(\theta)\sin(\theta) + mm'd^n_{om}(\theta)d^{n'}_{om'}(\theta)/\sin(\theta)]\times \\ &\times[\int_0^{2\pi} f^2_{mnm'n'}(\theta,\varphi)d\varphi] - \frac{n(n+1)}{x}d^n_{om}(\theta)b^{n'}_{om'}(\theta)\sin(\theta)[\int_0^{2\pi} f^3_{mnm'n'}(\theta,\varphi)d\varphi] - \\ &-i\frac{n'(n'+1)}{x_1}d^n_{om}(\theta)d^{n'}_{om'}(\theta)\sin(\theta)[\int_0^{2\pi} f^4_{mnm'n'}(\theta,\varphi)d\varphi]d\theta, \end{aligned} \tag{24}$$

$$\begin{aligned} I'^{21}_{mnm'n'} &= (-1)^{(m+m')}\int_0^{\pi} \frac{n'(n'+1)}{x_1}b^n_{om}(\theta)d^{n'}_{om'}(\theta)\sin(\theta)[\int_0^{2\pi} f^3_{mnm'n'}(\theta,\varphi)d\varphi] - \\ &-im\frac{n'(n'+1)}{x_1}d^n_{om}(\theta)d^{n'}_{om'}(\theta)/\sin(\theta)[\int_0^{2\pi} f^4_{mnm'n'}(\theta,\varphi)d\varphi] + \\ &+mm'd^n_{om}(\theta)d^{n'}_{om'}(\theta)/\sin(\theta) + \\ &+b^{n'}_{om}(\theta)b^{n'}_{om'}(\theta)\sin(\theta)[\int_0^{2\pi} f^5_{mnm'n'}(\theta,\varphi)d\varphi]d\theta, \end{aligned} \tag{25}$$

$$I'^{22}_{mnm'n'} = (-1)^{(m+m')}\int_0^{\pi} i[md^n_{om}(\theta)b^{n'}_{om'}(\theta) + m'd^{n'}_{om'}(\theta)b^n_{om}(\theta)]\times$$
$$\times[\int_0^{2\pi} f^6_{mnm'n'}(\theta,\varphi)d\varphi] +$$
$$+\frac{n'(n'+1)}{x_1}b^n_{om}(\theta)d^{n'}_{om'}(\theta)[\int_0^{2\pi} f^7_{mnm'n'}(\theta,\varphi)d\varphi] - \frac{n(n+1)}{x}d^n_{om}(\theta)b^{n'}_{om'}(\theta)\times \quad (26)$$
$$\times[\int_0^{2\pi} f^8_{mnm'n'}(\theta,\varphi)d\varphi] + im\frac{n'(n'+1)}{x_1}d^n_{om}(\theta)d^{n'}_{om'}(\theta)[\int_0^{2\pi} f^9_{mnm'n'}(\theta,\varphi)d\varphi] +$$
$$+im'\frac{n(n+1)}{x}d^n_{om}(\theta)d^{n'}_{om'}(\theta)[\int_0^{2\pi} f^{10}_{mnm'n'}(\theta,\varphi)d\varphi]d\theta,$$

$$c^1_{mnm'n'}(\theta,\varphi) = \exp(i\Delta_{m'm})h_n(x)j_n(x_1)r^2(\theta,\varphi),\ c^2_{mnm'n'}(\theta,\varphi) = \exp(i\Delta_{m'm})u_n(x)j_n(x_1)r^2(\theta,\varphi),$$
$$c^3_{mnm'n'}(\theta,\varphi) = \exp(i\Delta_{m'm})h_n(x)j_n(x_1)\frac{dr(\theta,\varphi)}{d\theta},\ c^4_{mnm'n'}(\theta,\varphi) = \exp(i\Delta_{m'm})u_n(x)j_n(x_1)\frac{dr(\theta,\varphi)}{d\theta},$$
$$c^3_{mnm'n'}(\theta,\varphi) = \exp(i\Delta_{m'm})h_n(x)j_n(x_1)\frac{dr(\theta,\varphi)}{d\theta},\ c^4_{mnm'n'}(\theta,\varphi) = \exp(i\Delta_{m'm})u_n(x)j_n(x_1)\frac{dr(\theta,\varphi)}{d\theta},$$
$$c^5_{mnm'n'}(\theta,\varphi) = \exp(i\Delta_{m'm})h_n(x)v_n(x_1)r^2(\theta,\varphi),\ c^6_{mnm'n'}(\theta,\varphi) = \exp(i\Delta_{m'm})u_n(x)v_n(x_1)r^2(\theta,\varphi),$$
$$c^7_{mnm'n'}(\theta,\varphi) = \exp(i\Delta_{m'm})u_n(x)j_n(x_1)\frac{dr(\theta,\varphi)}{d\varphi},\ c^8_{mnm'n'}(\theta,\varphi) = \exp(i\Delta_{m'm})h_n(x)v_n(x_1)\frac{dr(\theta,\varphi)}{d\varphi},$$
$$c^9_{mnm'n'}(\theta,\varphi) = \exp(i\Delta_{m'm})u_n(x)j_n(x_1)\frac{dr(\theta,\varphi)}{d\theta},\ c^{10}_{mnm'n'}(\theta,\varphi) = \exp(i\Delta_{m'm})h_n(x)v_n(x_1)\frac{dr(\theta,\varphi)}{d\theta},$$
$$f^1_{mnm'n'}(\theta,\varphi) = \exp(i\Delta_{m'm})j_n(x)j_n(x_1)r^2(\theta,\varphi),\ f^2_{mnm'n'}(\theta,\varphi) = \exp(i\Delta_{m'm})v_n(x)j_n(x_1)r^2(\theta,\varphi),$$
$$f^3_{mnm'n'}(\theta,\varphi) = \exp(i\Delta_{m'm})j_n(x)j_n(x_1)\frac{dr(\theta,\varphi)}{d\theta},\ f^4_{mnm'n'}(\theta,\varphi) = \exp(i\Delta_{m'm})u_n(x)j_n(x)j_n(x_1)\frac{dr(\theta,\varphi)}{d\theta},$$
$$f^5_{mnm'n'}(\theta,\varphi) = \exp(i\Delta_{m'm})v_n(x)j_n(x_1)r^2(\theta,\varphi),\ f^6_{mnm'n'}(\theta,\varphi) = \exp(i\Delta_{m'm})v_n(x)u_n(x_1)r^2(\theta,\varphi),$$
$$f^7_{mnm'n'}(\theta,\varphi) = \exp(i\Delta_{m'm})v_n(x)j_n(x_1)\frac{dr(\theta,\varphi)}{d\varphi},\ f^8_{mnm'n'}(\theta,\varphi) = \exp(i\Delta_{m'm})j_n(x)v_n(x_1)\frac{dr(\theta,\varphi)}{d\varphi},$$
$$f^9_{mnm'n'}(\theta,\varphi) = \exp(i\Delta_{m'm})v_n(x)j_n(x_1)\frac{dr(\theta,\varphi)}{d\theta},\ f^{10}_{mnm'n'}(\theta,\varphi) = \exp(i\Delta_{m'm})j_n(x)v_n(x_1)\frac{dr(\theta,\varphi)}{d\theta}.$$

Thus, by using the method of extended boundary conditions, a solution to the scattering problem is obtained for the case of an irregular shape of the scatterer (ellipsoid).

The expansion coefficients of the scattered and incident electromagnetic fields turn out to be related by linear transformations of the T-matrix. The latter depends on a number of parameters (the size of the scatterer with respect to the wavelength, the refractive index, etc.), but it is invariant with respect to the direction of propagation of incident radiation for the selected coordinate system.

It is also necessary to specify the complexity of the application of the *T*-matrix method for biological media with typical optical "softness". This complexity is associated (in the specified cases) with poor convergence of the series corresponding to them in the calculation formulas for the elements of the *T*-matrix. The possibility of highly oscillating behavior of the integrand may also reduce accuracy. Moreover, the numerical inversion of the matrix will be poorly conditioned for scatterers with a zero (or small) imaginary part of the refractive index.

Following [22, 23], convergence can be significantly improved if the so-called LU factorization based on the application of an extended boundary condition is used. The graphs shown in Fig. 1 confirm the validity of this statement.

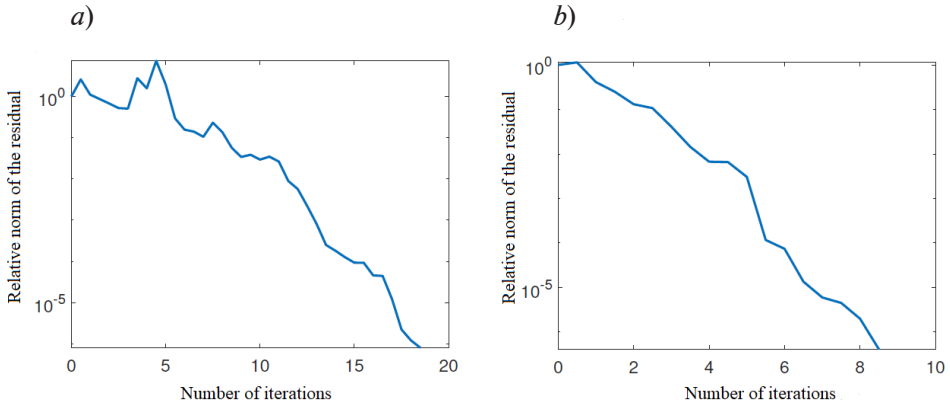

Fig. 1. Dependences of relative residual norm on the iteration number for the distances of 1 μm (*a*) and 2 μm (*b*) between particles
The dependences were btained using the method of biconjugate gradients with preconditioning (see Table 1)

Table 1

Parameters of model medium including 5 particles

Distance between particles, μm	Refractive index for particle		
	m_1	m_2	m_3, m_4, m_5
1	1.37	1.34	1.33
2	1.35	1.33	

Note. a = 18 μm, c = 3 μm for the first three particles, a = 5 μm, c = 5 μm (a are the lengths of the semi-axes of the spheroid along the x, y axes, respectively, and c are the lengths along the z axis).

Multiple scattering by ensembles of nonspherical scatterers

Electromagnetic waves incident on the surface of the jth scatterer form a field $\mathrm{E}_i(j)$, which consists of two components: the field created initially by incident waves and the field created by scattering by an ensemble of particles. The sum of the terms follows the expression

$$\mathbf{E}_i(j) = \mathbf{E}_0(j) + \sum_{i \neq j} \mathbf{E}_s(l, j). \tag{27}$$

A group of fields scattered by the jth particle is contained under the summation sign; (l,j) assigns the conversion from the coordinate system l to the coordinate system j.

Let us write out an expression for the incident field separately:

$$\mathbf{E}_0 = -\sum_{n=1}^{\infty} \sum_{m=-n}^{n} iE_{mn} \left[p_{mn}^{j_0,j} \mathbf{N}_{mn}^1(kr) + q_{mn}^{j_0,j} \mathbf{M}_{mn}^1(kr) \frac{e^{im\phi}}{kr} \right]. \tag{28}$$

Note that the incidence of waves relative to the center of each jth particle in its coordinate system (j-system) is considered.

The expansion coefficients for the given plane electromagnetic wave take the following form [18]:

$$p_{mn}^{j_0,j} = 4\pi(-1)^m i^n d_n \mathbf{C}_{mn}^*(\theta_{ink}) \mathbf{E}_{ink}(\mathbf{k}_{ink}, \mathbf{r}_{j_0,j}) \exp(-im\varphi_{ink}),$$

$$q_{mn}^{j_0,j} = 4\pi(-1)^m i^{n-1} d_n \mathbf{B}^*_{mn}(\theta_{ink})\mathbf{E}_{ink}(\mathbf{k}_{ink}, \mathbf{r}_{j_0,j}) \exp(-im\varphi_{inc}).$$

The complex conjugation is marked with an asterisk as standard, the notation $\mathbf{E}_{ink}(\mathbf{k}_{ink},\mathbf{r}_{j_0,j})$ represents the vector of linear polarization.

The following expression holds true for a field scattered by particles:

$$\mathbf{E}_s = -\sum_{n=1}^{\infty}\sum_{m=-n}^{n} iE_{mn}\left[p_{mn}^{l,j}\mathbf{N}_{mn}^1 + q_{mn}^{l,j}\mathbf{M}_{mn}^1\right], \tag{29}$$

where the expansion coefficients have the form [19].

The next stage consists in constructing an infinite system of algebraic equations based on combining expressions (27)–(29), taking into account expressions (16) for each *j*th particle of arbitrary shape:

$$\begin{pmatrix} a^j \\ b^j \end{pmatrix} = T_{12}^j\left[\begin{pmatrix} p^{i,j} \\ q^{i,j} \end{pmatrix} + \sum_{l\neq j}\begin{pmatrix} A(l,j) & B(l,j) \\ B(l,j) & A(l,j) \end{pmatrix}\begin{pmatrix} a^j \\ b^j \end{pmatrix}\right]. \tag{30}$$

The corresponding coefficients are determined in [19].

To solve the given system, we settled on the reduction method followed by the application of the biconjugate gradient method.

After the coefficients of system (30) are found, it becomes possible to record the total field in the far zone:

$$E_{totalq} = \sum_{n=1}^{\infty}\sum_{m=-n}^{n} iE_{mn}\left[a_{mn}\mathbf{N}_{mn}^3 + b_{mn}\mathbf{M}_{mn}^3\right], \tag{31}$$

$$a_{mn} = \sum_{j=1}^{L}\exp(-i\mathbf{k}_s,\mathbf{r}_j)a_{mn}^j,\ b_{mn} = \sum_{j=1}^{L}\exp(-i\mathbf{k}_s,\mathbf{r}_j)b_{mn}^j. \tag{32}$$

The componentwise notation of the scattered field has the form:

$$E_{s\theta} \sim \sum_{n=1}^{\infty}\sum_{m=-n}^{n}(-i)^n E_{mn} i\left[a_{mn}\tau_{mn} + b_{mn}\pi_{mn}\right]\frac{\exp(ikr)}{ikr}\exp(im\varphi), \tag{33}$$

$$E_{s\varphi} \sim \sum_{n=1}^{\infty}\sum_{m=-n}^{n}(-i)^n E_{mn} i\left[a_{mn}\pi_{mn} + b_{mn}\tau_{mn}\right]\frac{\exp(ikr)}{ikr}\exp(im\varphi), \tag{34}$$

where the functions of the angle follow the expressions

$$\tau_{mn} = \frac{\partial}{\partial\theta}P_n^m(\cos\theta),\ \pi_{mn} = \frac{m}{\sin\theta}P_n^m(\cos\theta).$$

The tilde sign (~) here implies the use of an asymptotic approximation.

Moreover, since we believe that scattering processes are considered at sufficiently large distances from the particle, where the electric vectors of the scattered and incident fields can be considered parallel, we can further simplify expressions (33) and (34) (we believe that only the component θ is nonzero in the far zone).

$$E_{s\theta} \sim E_0\frac{\exp(ikr)}{-ikr}\sum_{n=1}^{\infty}\sum_{m=-n}^{n}\frac{2n+1}{n(n+1)}(a_{mn}\tau_{mn} + b_{mn}\pi_{mn}), \tag{35}$$

$$E_{s\varphi} \sim E_0\frac{\exp(ikr)}{-ikr}\sum_{n=1}^{\infty}\sum_{m=-n}^{n}\frac{2n+1}{n(n+1)}(a_{mn}\pi_{mn} + b_{mn}\tau_{mn}), \tag{36}$$

$$\tau_n = \frac{\partial}{\partial\theta}P_n(\cos\theta),\ \pi_n = \frac{1}{\sin\theta}P_n(\cos\theta).$$

Simulation of the reflection of a plane wave from a nontrivial multilayered structure

Consider a nontrivial layered structure (nontriviality here is understood as waviness of the layers), where each layer has its own refractive index, and use some of the results obtained in [20].

A flat *p*-polarized wave (a similar case of *s*-polarization would be simpler) is incident on the model considered at an angle θ. Our goal is to find the reflected field. Let us write out expressions for the fields formed by light radiation passing through the above layers and reflected from them, assuming that the phases of the waves oscillate rapidly, and the amplitudes change slowly:

$$E_1 = \exp(\frac{i}{\varepsilon}\tau_{inc}(\xi_1,\xi_2,\xi_3)) + \exp(\frac{i}{\varepsilon}\tau_{1ref}(\xi_1,\xi_2,\xi_3))\,\mathrm{A}(\xi_1,\xi_2,\xi_3,\varepsilon_x,\varepsilon_y), \tag{37}$$

$$E_2 = \exp(\frac{i}{\varepsilon}\tau_{2elap}(\xi_1,\xi_2,\xi_3))\,\mathrm{B}^+(\xi_1,\xi_2,\xi_3,\varepsilon_x,\varepsilon_y) + \\ + \exp(\frac{i}{\varepsilon}\tau_{3ref}(\xi_1,\xi_2,\xi_3))\,\mathrm{B}^-(\xi_1,\xi_2,\xi_3,\varepsilon_x,\varepsilon_y), \tag{38}$$

$$E_3 = \exp(\frac{i}{\varepsilon}\tau_{3elap}(\xi_1,\xi_2,\xi_3))\,\mathrm{C}^+(\xi_1,\xi_2,\xi_3,\varepsilon_x,\varepsilon_y) + \\ + \exp(\frac{i}{\varepsilon}\tau_{3ref}(\xi_1,\xi_2,\xi_3))\,\mathrm{C}^-(\xi_1,\xi_2,\xi_3,\varepsilon_x,\varepsilon_y), \tag{39}$$

$$E_4 = \exp(\frac{i}{\varepsilon}\tau_{4elap}(\xi_1,\xi_2,\xi_3))\,\mathrm{D}^+(\xi_1,\xi_2,\xi_3,\varepsilon_x,\varepsilon_y) + \\ + \exp(\frac{i}{\varepsilon}\tau_{5ref}(\xi_1,\xi_2,\xi_3))\,\mathrm{D}^-(\xi_1,\xi_2,\xi_3,\varepsilon_x,\varepsilon_y) + E_{4scat\phi}(\xi_1,\xi_2,\xi_3), \tag{40}$$

$$E_5 = \exp(\frac{i}{\varepsilon}\tau_{5elap}(\xi_1,\xi_2,\xi_3))E(\xi_1,\xi_2,\xi_3,\varepsilon_x,\varepsilon_y). \tag{41}$$

Similar to our earlier study [20], we sequentially found the terms of the series for the required amplitudes, as well as the expression for the Gaussian beam.

Distribution function for particles simulated by ellipsoids of revolution

Let us determine the parameters of the model medium corresponding to normal human skin (Table 2).

Let the incident plane wave propagate in the *x*-axis direction (the semi-minor axis for an oblate ellipsoid) and have polarization in the *z*-axis direction.

Fig. 2 shows images of oblate and prolate ellipsoids and the coordinate system used associated with them.

The model medium is as close as possible to the real parameters of normal human skin.

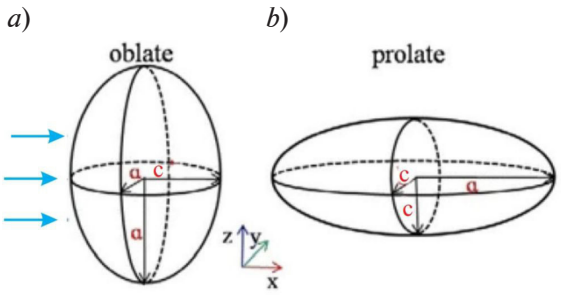

Fig. 2. Images of oblate (*a*) and prolate (*b*) ellipsoids;
a, *c* are the lengths of their semi-axes directed along the corresponding coordinate axes.
Blue arrows indicate the direction of the incident laser beams

Table 2

Adopted characteristics of the model medium [20]

Parameter	Notation	Parameter value for layer i		
		(2)	(3)	(4)
Layer thickness, μm	d_i	65	565	90
Set of distortion parameters	a_i	–0.0024	0.021	0.041
	b_i	0.0200	0.030	0.050
	c_i	0.010		
Refractive index (real part)	n_i^0	1.50	1.40	1.35

Notes. 1. Distortion parameters are represented by the formula $H_i = c_i \sin(a_i x + b_i y)$.
2. Refractive index of ambient air $n_1 = 1{,}000$; we assumed $\chi_2 = \chi_3 = \chi_4 = \chi_5 = 10^{-5}$; $n_5^0 = 1.40$ for the ith layer of the model absorbing medium with $n_i = n_i^0 + i\chi_i$.

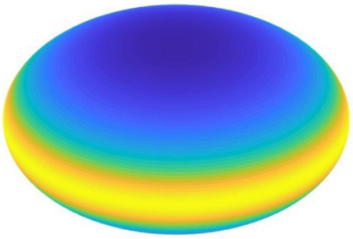

Fig. 3. General view of oblate ellipsoid under consideration with dimensions a = 18 μm, c = 3 μm

A number of well-known facts allow us to consider the erythrocyte as a homogeneous scatterer: the erythrocyte membrane is thin and does not significantly affect the scattering of laser radiation, and cellular organelles are not included in the structure of the erythrocyte. Thus, our calculations are performed for an oblate ellipsoid (Fig. 3).

The mathematical approach we developed allows to detect the aggregation of particles as well as to determine their spectral parameters for the *in vivo* case. The illustrations presented below (Figs. 4–6) demonstrate the capabilities of the software package we created by based on the presented theoretical approach. Evidently, both the numerical parameters and the shapes of the curves change with varying distances between the scatterers.

The results obtained indicate the difference in cell sizes, the diversity of their internal structures, and the effect of interference on the pattern of wave fields scattered by neighboring particles.

Thus, the developed method creates new possibilities, allowing to take into account the effects of cooperative interaction of particles in the case of denser packing of erythrocytes.

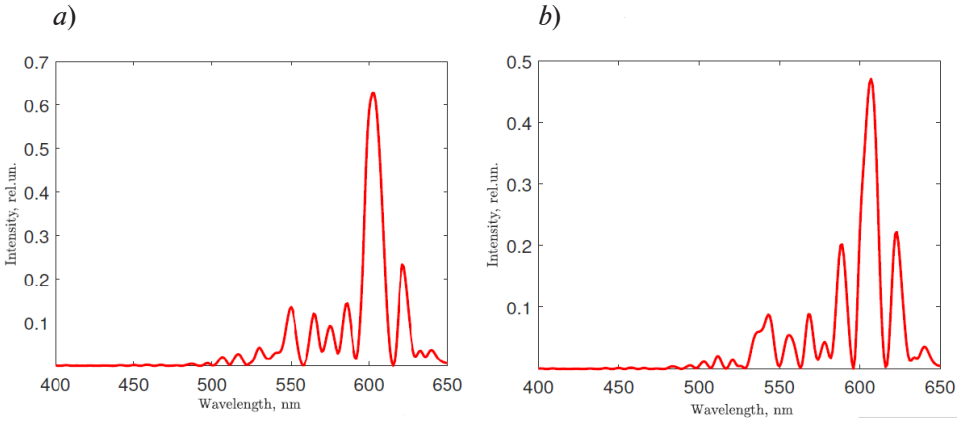

Fig. 4. Functional dependences of intensity versus wavelength for the light scattered by particle ensembles located in the layer; distances between the particles are 1 μm (*a*) and 2 μm (*b*) (see Table 1)

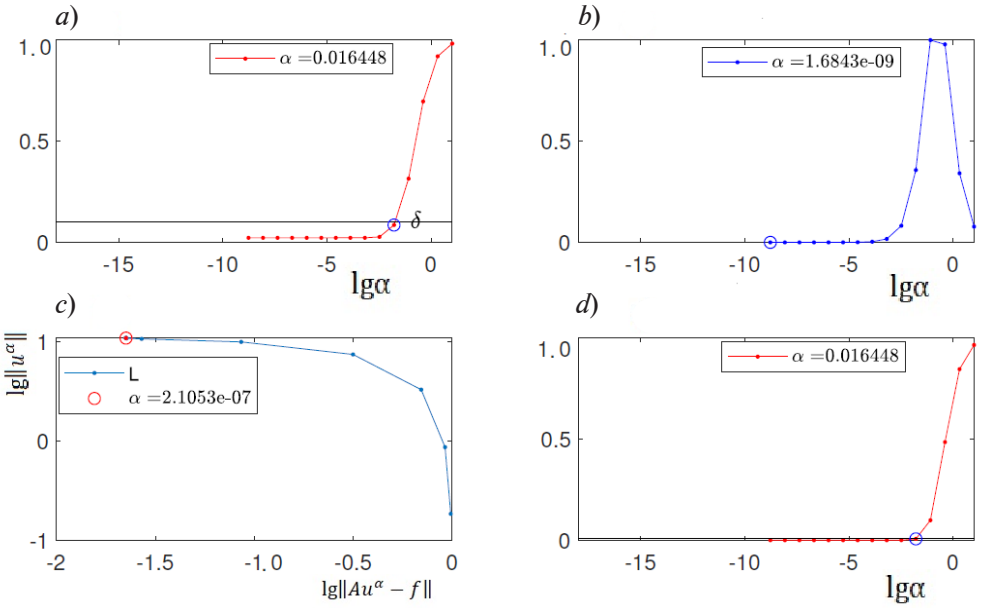

Fig. 5. Results of automatic determination of regularization parameter α from the given kernel errors and "measured" data using different criteria: residual (*a*), quasi-optimality (*b*), *L*-curve (*c*) and generalized residual principle (*d*) for a bimodal distribution (see Fig. 7,*a*)

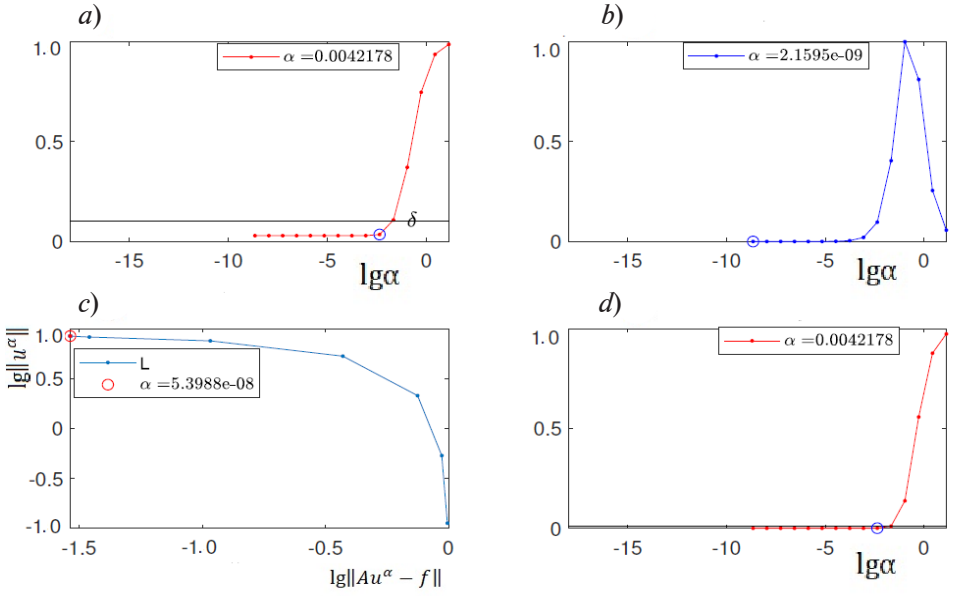

Fig. 6. Results similar to those shown in Fig. 5, but for normal distribution (see Fig. 7,*b*)

The next stage of the study consists of solving the inverse problem: to find the distribution of erythrocytes (assuming them to be spheroids) from the aspect ratio of the spheroid ($\rho = a/c$), based on the known intensity of laser radiation scattering (measured with some error) by an aggregated ensemble of particles located in the layer (*in vivo* case).

Such problems are described by linear first-kind Fredholm integral equations, taking the form

$$\boldsymbol{Au} \equiv \int_{\rho\min}^{\rho\max} I_{scat(\theta)}(\rho,\lambda)u(\rho)d\rho = f(\lambda), \tag{42}$$

where $\boldsymbol{A}$ is the integral operator, $I_{scat(\theta)}(\rho,\lambda)$ is the kernel of the integral equation, $u(\rho)$ is the required cell size distribution, $f(\lambda) \equiv I_{blood}(\theta,\lambda)$ is the scattering intensity.

The kernel $I_{scat(\theta)}(\rho,\lambda)$ is defined as the intensity of light scattered in the direction of the angle θ (the angle is chosen experimentally) by a nonspherical particle (see Eq. (35)). We assume that this kernel is a function continuous in the rectangle $\Omega = ([c,d]\times[a,b])$, and $f(\lambda) \in L_{[c,d]}$ ($a \equiv \rho_{\min}$, $b \equiv \rho_{\max}$, $c \equiv \lambda_{\min}$, $d \equiv \lambda_{\max}$).

The inversion of the integral operator $\boldsymbol{A}$ for the inverse problem (see equation (42)) is unstable, therefore, it is advisable to use the Tikhonov regularization method for the numerical solution [24, 25].

Automatic determination of the regularization parameter based on the given kernel errors and "measured" data is possible within the framework of the software package we developed. (This package includes the methods of relative residual, the generalized residual principle (GRP), the L-curve method and the quasi-optimality criterion.)

Thus, we propose to choose the regularization parameter in accordance with several criteria. In a problem with a known model solution, this allows us to find the range of the best values of the parameter α. It turned out that the residual principle and the GRP gave the same parameter value and when they were used to solve the integral equation (42), a profile close to the model was reconstructed.

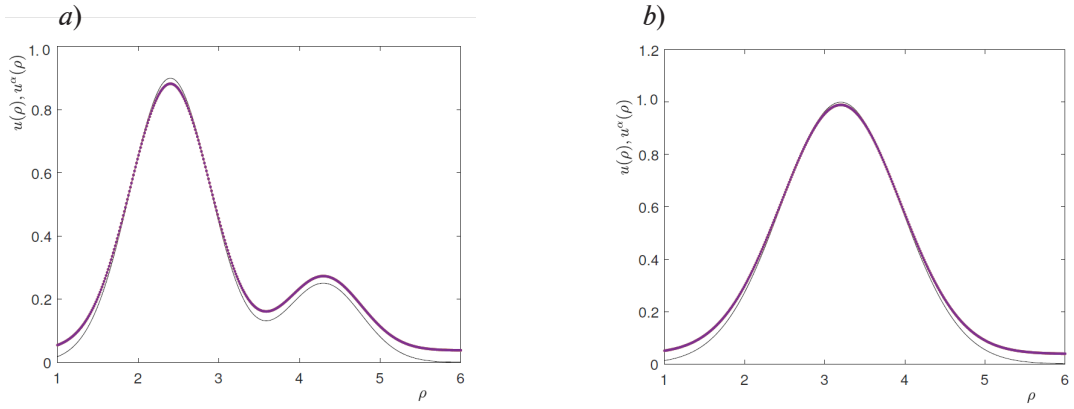

Fig. 7. Bimodal (*a*) and normal (*b*) size distributions for spheroidal particles with two values of the distance between the scatterers: 1 μm (*a*) and 2 μm (*b*). Graphs of functions from [26] (solid lines) are compared with the results of our numerical solution (dotted lines)

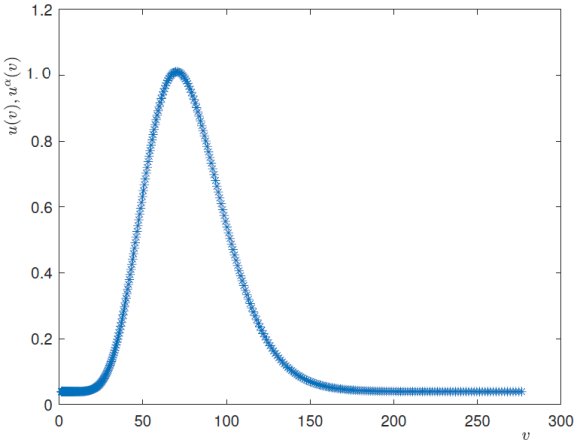

Fig. 8. Case of normal volume distribution of the particles (Price–Jones curve) obtained for distance of 2 μm between the scatterers

Fig. 7,*a* shows a comparison of the two curves. The solid black curve corresponds to an asymmetric bimodal particle size distribution, which is predefined by the function from [26]. The given distribution simulates the presence of fractions of normocytes and macrocytes. The dotted colored curve corresponds to our numerical solution of the problem and demonstrates that both peaks of the size distribution were reconstructed quite satisfactorily. A similar solid curve in Fig. 7,*b* also corresponds to a predefined size distribution, a normal one (see [26]). As a result of our numerical solution of the problem (dotted colored curve), where the noise level in the right-hand side of equation (42) is assumed to be 5%, a completely satisfactory agreement with the given function is also obtained. Thus, the particle size distribution profiles were reconstructed with high accuracy.

The analysis of the graphs in Fig. 7 also allows to conclude that taking into account the nonsphericity of particles accurately reconstructs the Price–Jones curve (Fig. 8), describing the typical volume distribution of human blood corpuscles.

Erythrocyte indices

In this section, we consider the numerical evaluation of erythrocyte indices (which are standard in clinical practice), in particular the mean corpuscular volume (MCV) and the degrees of dispersion of red blood cells by volume. These include the deviations of the relative distribution of erythrocytes over the volume (red cell distribution width, abbreviated as RDW) from the mean (coefficient of variation, or CV) and from the standard (standard deviation, or SD).

In other words, RDW-CV shows a percentage deviation of the erythrocyte volume from the mean, and RDW-SD is the difference between the largest and smallest erythrocyte (measured in femtoliters, like MCV).

Let us first determine the volume of the body formed by revolution around the axis of the shape:

$$V_{rot} = 4\pi\int_0^1 xy(x)dx, \tag{43}$$

where y(x) represents the family of Perseus curves [27]

$$y(x) = \mathrm{c}\sqrt{a^2 - (\sqrt{x^2 - p^2} - d^2)^2}; \tag{44}$$

the following shape parameters are given here: a, b are the semi-axes of the ellipse, $c = a/b$ (a = 0.150662, c = 1.659376); d is the distance from the origin to the center of the ellipse (d = 1.768398); p is the distance from the axis of the torus to the secant plane (p = 1.637922). Expression (44) defines families of Perseus curves. They are lines of intersection of the surface of the torus with planes parallel to its axis, and represent algebraic lines of the 4th order.

The volume of revolution for this shape is

$$V_{rot} = 4\pi\int_0^1 xc\sqrt{a^2 - (\sqrt{x^2 + p^2} - d)^2}\,dx = 1.2799.$$

If we assume that the diameter of a human erythrocyte is 7.55 μm on average, then the relationship between the volume and the radius of the erythrocyte takes the form $V_{\mathrm{MCV}} = V_{rot}R^3$ and the mean volume of the erythrocyte is V_{MCV} = 1.2799·68.8536 μm^3.

The equation of the form (44) is written in a spherical coordinate system:

$$r^4\alpha_1 - 2r^2\alpha_2 - \beta_2 = 0,$$

and the corresponding solution of this biquadratic equation has the form

$$r(\theta,\varphi) = \frac{\sqrt{\alpha_1(-\alpha_2 + \sqrt{\alpha_1\beta_2 + \alpha_2^2})}}{\alpha_1}, \tag{45}$$

where $\alpha_1 = \sin^2\theta\gamma_1,\ \alpha_2 = \sin\theta\beta_1,\ \beta_2 = \frac{2db^2}{a^2}p - \gamma_2;$
here

$$\gamma_1 = \sin^2\varphi + \frac{b^2}{a^2}\cos^2\varphi,\ \gamma_2 = b^2(1+\frac{p}{a^2}) - d^2,\ \beta_1 = \gamma_1\gamma_2 - \frac{db^2}{a^2}\cos^2\varphi.$$

Solving the inverse problem allows to find the volume distribution function (see Fig. 8) taking into account the equation of the surface (45).

We should note that similar results were obtained in [29].

In this case, it is possible to calculate the size heterogeneity index of the erythrocyte based on the obtained theoretical volume distribution.

In medical practice, the RDW-SD indicator is the result of direct measurement of the width of the erythrocyte curve at a 20% level (with the height of the curve taken as 100%) [28].

For example, RDW-SD = 118 − 36 = 82 fl. Then values within the range of 80−100 fl characterize the erythrocyte as a normocyte, below 80 fl as a microcyte, and above 100 fl as a macrocyte.

Notably, the RDW-SD indicator is more sensitive to the appearance of a certain number of micro- and macrocytes in the erythrocyte population, since it is measured at the lower part of the erythrocyte volume distribution curve. If reticulocytosis occurs (an increase in reticulocytes (precursors of erythrocytes) in the process of hematopoiesis), this indicator changes faster, since there is a certain broadening of the erythrocyte curve.

Results and conclusions

The main goal of the study was to develop and refine an electrodynamic model of the interaction of low-power laser radiation with a dispersed medium, including elements of irregular shape (ellipsoid), which are models of blood cells (erythrocytes) located in a medium with a layered structure (*in vivo* case).

Let us overview our main findings.

1. The developed analytical methods for calculating the light scattering characteristics of particles located in a layered medium are described. It is assumed that these particles are arbitrarily oriented and have an irregular shape (nonspherical).

2. Steps were taken to optimize the convergence of processes using the method of extended boundary conditions; this increased the possibilities of using the *T*-matrix method.

3. The mathematical model developed for the analysis of biological processes based on calculated optical characteristics was implemented in a new software package.

4. The developed approach to the problem made it possible to correctly reconstruct the traditionally used indicator of the distribution of blood corpuscles (RDW-SD) for the *in vivo* case, taking into account the aspect ratios and the structural features of the biological aggregate.

5. We found an approach to theoretically predicting the number of abnormally sized erythrocytes in a biological material using the developed model, based on the standard measurement of the width of the size distribution of erythrocytes. For example, in the case of the presence of micro- and macrocytes, it is possible to diagnose the degree of anicytosis, since the width of the distribution is higher than the reference value, and the obtained curves of the volume distribution of erythrocytes clearly indicate the difference in cell size.

Thus, the RDW index is an informative and convenient marker for laboratory diagnostics.

The results obtained serve as the basis for the proposed new method of rapid analysis of whole blood. According to this method, it is necessary to find the distributions of bloody corpuscles by characteristic indices, the RDW index as well as the geometric characteristics of red blood cells related to their volume and shape, for the *in vivo* case.

REFERENCES

1. **Tuchin V. V.,** Handbook of optical biomedical diagnostics, 2nd Edition, Vol. 1: Light-tissue interaction, SPIE Press, Bellingham, WA, USA, 2016.

2. **Eremina E., Eremin Y., Wriedt T.,** Analysis of light scattering by erythrocyte based on the discrete sources method, Opt. Commun. 244 (1–6) (2005) 15–23.

3. **Eremina E., Hellmers J., Eremin Y., Wriedt T.,** Different shape models for erythrocyte: Light scattering analysis based on the discrete sources method, J. Quant. Spectrosc. Radiat. Transfer. 102 (1) (2006) 3–10.

4. **Eremina E., Wriedt T.,** Light scattering analysis by a particle of extreme shape via discrete soused method, J. Quant. Spectrosc. Radiat. Transfer. 89 (1–4) (2004) 67–77.

5. **Mishchenko M. I., Wiscomber W. J., Hovenier J. W., Travis L. D.,** Overview of scattering by nonspherical particles, In book: Mishchenko M. I., Hovenier J. W., Travis L. D. (Eds.), Light scattering by nonspherical particles: Theory, measurements and applications, Academic Press, Cambridge, Massachusetts, USA (1999) 29–60.

6. **Latimer P.,** Light scattering by ellipsoids, J. Colloid Interface Sci. 53 (1) (1975) 102–109.

7. **Cai Q., Liou K.-N.,** Polarized light scattering by hexagonal ice crystals: Theory, Appl. Opt. 21 (19) (1982) 3569–3580.

8. **Hammer M., Schweitzer D., Michel B., et al.,** Single scattering by red blood cells, Appl. Opt. 37 (31) (1998) 7410–7418.

9. **Van de Hulst H. C.,** Light scattering by small particles, John Willey & Sons Inc., New York, 1957.

10. **Shatilov A. V.,** O rasseyanii sveta dielektricheskimi ellipsoidami, sravnimymi s dlinoyvolny. 1. Obshchee vyrazheniye dlya indikatrisy rasseyaniya ellipsoidalnoy chastitsy [About light scattering by dielectric ellipsoids comparable to the wavelength. 1. General expression for the scattering indicatrix of an ellipsoidal particle], Optika i Spektroskopiya. 9 (1) (1960) 86–91 (in Russian).

11. **Newton R. G.,** Scattering theory of waves and particles, Second Edition (Dover Books on Physics), Dover Publications, New York, 2013.

12. **Klett J. D., Sutherland R. A.,** Approximate methods for modeling the scattering properties of nonspherical particles: Evaluation of the Wentzel–Kramers–Brillouin method, Appl. Opt. 31 (3) (1992) 373–386.

13. **Erma V. A.,** An exact solution for the scattering of electromagnetic waves from bodies of arbitrary shape: III. Obstacles with arbitrary electromagnetic properties, Phys. Rev. 179 (5) (1969) 1238–1246.

14. **Waterman P. C.,** Matrix formulation of electromagnetic scattering, Proc. IEEE. 53 (8) (1969) 805–812.

15. **Waterman P. C.,** Symmetry, unitarity and geometry in electromagnetic scattering, Phys. Rev. D. 3 (4) (1971) 825–839.

16. **Steinke J. M., Shepherd A. P.,** Comparison of Mie theory and light scattering of red blood cells, Appl. Opt. 27 (19) (1988) 4027–4033.

17. **Yaroslavsky A. N., Goldbach T., Schwarzmaier H.,** Influence of the scattering phase function approximation on the optical properties of blood determined from the integrating sphere measurements, J. Biomed. Opt. 4 (1) (1999) 47–53.

18. **Tsang L., Kong J. A., Shin R. T.,** Theory of microwave remote sensing, Willey Interscience, New York, 1985.

19. **Kulikov K. G., Radin A. M.,** Study of dispersion and absorption of an ensemble of spherical particles inside an optical cavity and new possibilities of predicting the optical characteristics of biological media by intracavity spectroscopy, Opt. Spectrosc. 92 (2) (2002) 199–206.

20. **Golovitskii A. P., Kontsevaya V. G., Kulikov K. G.,** An electrodynamic model for determining the distribution function of particles by size for blood cells *in vivo*, St. Petersburg State Polytechnical University Journal. Physics and Mathematics. 16 (1) (2023) 97–110 (in Russian).

21. **Doicu A., Wriedt T., Eremin Y. A.,** Light scattering by systems of particles. Null-field method with discrete sources: Theory and programs, Springer, Berlin, New York, 2006.

22. **Mishchenko M. I., Travis L. D.,** T-matrix computations of light scattering by large spheroidal particles, Opt. Commun. 109 (1–2) (1994) 16–21.

23. **Mishchenko M. I., Travis L. D.,** Capabilities limitations of a current FORTRAN implementation of the T-matrix method for randomly oriented, rotationally symmetric scatterers, J. Quant. Spectrosc. Radiat. Transfer. 60 (3) (1998) 309–324.

24. **Tikhonov A. N., Arsenin V. A.,** Solution of ill-posed problems, Winston, USA, 1977.

25. **Tikhonov A. N., Goncharsky A. V., Stepanov V. V., Yagola A. G.,** Numerical methods for the solution of ill-posed problems, Book Series: Mathematics and its Applications, Vol. 328, Springer Dordrecht, Netherlands, 1995.

26. **Ustinov V. D.,** On inverse reconstruction problems of the erythrocyte size distribution in laser diffractometry, Math. Models Comput. Simul. 9 (5) (2017) 561–569.

27. **Zub V. V., Kirillov V. Kh., Kuzakon V. M.,** Geometriya eritrotsita [Erythrocyte geometry], Sci. Works. (48) (2015) 182–186 (in Russian).

28. **Caporal F. A., Comar S. R.,** Evaluation of RCW-CV, RDW-SD, and MATH-1SD for the detection of erythrocyte anisocytosis observed by optical microscopy, J. Bras. Pathol. Med. Lab. 49 (5) (2013) 324–331.

29. **Doubrovski V. A., Torbin S. O., Zabenkov I. V.,** Determination of individual and average characteristics of native blood erythrocytes by the static spectral digital microscopy method, Opt. Spectrosc. 130 (6) (2022) 709–719.

СПИСОК ЛИТЕРАТУРЫ

1. **Тучин В. В.** Оптическая биомедицинская диагностика. В 2 тт. Т. 1. М.: Ай Пи Ар Медиа, 2021.549 с.

2. **Eremina E., EreminY., Wriedt T.** Analysis of light scattering by erythrocyte based on the discrete sources method // Optics Communications. 2005. Vol. 244. No. 1–6. Pp. 15–23.

3. **Eremina E., Hellmers J., EreminY., Wriedt T.** Different shape models for erythrocyte: Light scattering analysis based on the discrete sources method // Journal of Quantitative Spectroscopy and Radiative Transfer. 2006. Vol. 102. No. 1. Pp. 3–10.

4. **Eremina E., Wriedt T.** Light scattering analysis by a particle of extreme shape via discrete soused method // Journal of Quantitative Spectroscopy and Radiative Transfer. 2004. Vol. 89. No.1–4. Pp. 67–77.

5. **Mishchenko M.I., Wiscomber W. J., Hovenier J. W., Travis L. D.** Overview of scattering by nonspherical particles // Mishchenko M. I., Hovenier J. W., Travis L. D. (Eds.). Light scattering by nonspherical particles: Theory, measurements and applications. Cambridge, Massachusetts, USA: Academic Press, 1999. Pp. 29–60.

6. **Latimer P.** Light scattering by ellipsoids // Journal of Colloid and Interface Science. 1975. Vol. 53. No. 1. Pp. 102–109.

7. **Cai Q., Liou K.-N.** Polarized light scattering by hexagonal ice crystals: Theory // Applied Optics. 1982. Vol. 21. No. 19. Pp. 3569–3580.

8. **Hammer M., Schweitzer D., Michel B., Thamm E., Kolb A.** Single scattering by red blood cells // Applied Optics. 1998. Vol. 37. No. 31. Pp. 7410–7418.

9. **Ван де Хюлст Г.** Рассеяние света малыми частицами: Пер. с англ. М.: Изд-во иностр. лит-ры, 1961. 536 с.

10. **Шатилов А. В.** О рассеянии света диэлектрическими эллипсоидами, сравнимыми с длиной волны. 1. Общее выражение для индикатрисы рассеяния эллипсоидальной частицы // Оптика и спектроскопия. 1960. Т. 9. № 1. С. 86–91.

11. **Ньютон Р.** Теория рассеяния волн и частиц. Пер. с англ. М.: Мир, 1969. 600 с.

12. **Klett J. D., Sutherland R. A.** Approximate methods for modeling the scattering properties of nonspherical particles: Evaluation of the Wentzel –Kramers – Brillouin method // Applied Optics. 1992. Vol. 31. No. 3. Pp. 373–386.

13. **Erma V. A.** An exact solution for the scattering of electromagnetic waves from bodies of arbitrary shape: III. Obstacles with arbitrary electromagnetic properties // Physical Review. 1969. Vol. 179. No. 5. Pp.1238–1246.

14. **Waterman P. C.** Matrix formulation of electromagnetic scattering // Proceedings of the IEEE. 1969. Vol. 53. No. 8. Pp. 805–812.

15. **Waterman P. C.** Symmetry, unitarity and geometry in electromagnetic scattering // Physical Review D. 1971. Vol. 3. No. 4. Pp. 825–839.

16. **Steinke J. M., Shepherd A. P.** Comparison of Mie theory and light scattering of red blood cells // Applied Optics. 1988. Vol. 27. No. 19. Pp. 4027–4033.

17. **Yaroslavsky A. N., Goldbach T., Schwarzmaier H.** Influence of the scattering phase function approximation on the optical properties of blood determined from the integrating sphere measurements // Journal of Biomedical Optics. 1999. Vol. 4. No. 1. Pp. 47–53.

18. **Tsang L., Kong J. A., Shin R. T.** Theory of microwave remote sensing. New York: Willey Interscience, 1985. 632 p.

19. **Куликов К. Г., Радин А. М.** Исследование дисперсии и спектра поглощения совокупности сферических частиц в полости оптического резонатора и новые возможности прогноза оптических характеристик биологических сред методом внутрирезонаторной лазерной спектроскопии // Оптика и спектроскопия. 2002. Т. 92. № 2. С. 228–236.

20. **Головицкий А. П., Концевая В. Г., Куликов К. Г.** Электродинамическая модель определения функции распределения частиц по размерам для клеток крови (случай *in vivo*) // Научно-технические ведомости СПбГПУ. Физико-математические науки. 2023. Т. 16. № 1. С. 97–110.

21. **Doicu A., Wriedt T., Eremin Y. A.** Light scattering by systems of particles. Null-field method with discrete sources: Theory and programs. Berlin, New York: Springer, 2006. 322 p.

22. **Mishchenko M. I., Travis L. D.** T-matrix computations of light scattering by large spheroidal particles // Optics Communications. 1994. Vol. 109. No. 1–2. Pp. 16–21.

23. **Mishchenko M. I., Travis L. D.** Capabilities limitations of a current FORTRAN implementation of the T-matrix method for randomly oriented, rotationally symmetric scatterers // Journal of Quantative Spectroscopy and Radiative Transfer. 1998. Vol. 60. No. 3. Pp. 309–324.

24. **Тихонов А. Н., Арсенин В. А.** Методы решения некорректных задач. М.: Наука, 1979. 288 с.

25. **Тихонов А. Н., Гончарский А. В., Степанов В. В., Ягола А. Г.** Численные методы решения некорректных задач. М.: Наука, 1990. 232 с.

26. **Устинов В. Д.** Об обратных задачах восстановления распределения эритроцитов по размерам в лазерной дифрактометрии // Математическое моделирование. 2017. Т. 29. № 3. С. 51–62.

27. **Зуб В. В., Кириллов В. Х., Кузаконь В. М.** Геометрия эритроцита // Scientific Works. 2015. No. 48. Pp. 182–186.

28. **Caporal F. A., Comar S. R.** Evaluation of RCW-CV, RDW-SD, and MATH-1SD for the detection of erythrocyte anisocytosis observed by optical microscopy // Brazilian Journal of Pathology and Laboratory Medicine. 2013.Vol. 49. No. 5. Pp. 324–331.

29. **Дубровский В. А., Торбин С. О., Забенков И. В.** Определение индивидуальных средних характеристик эритроцитов нативной крови методом статистической цифровой спектральной микроскопии // Оптика и спектроскопия. 2022. Т. 130. № 6. С. 894–905.

THE AUTHORS

GOLOVITSKII Alexander P.
Peter the Great St. Petersburg Polytechnic University
29 Politechnicheskaya St., St. Petersburg, 195251, Russia
alexandergolovitski@yahoo.com
ORCID: 0000-0003-4292-0959

KONTSEVAYA Vera G.
Pskov State University
Peter the Great St. Petersburg Polytechnic University
2 Lenin Sq., Pskov, 180000, Russia
nkoncevoi@mail.ru
ORCID: 0000-0002-1434-5056

KULIKOV Kirill G.
Peter the Great St. Petersburg Polytechnic University
29 Politechnicheskaya St., St. Petersburg, 195251, Russia
kulikov.kirill.g@gmail.com
ORCID: 0000-0002-4610-7394

KOSHLAN Tatiana V.
St. Petersburg State University
7–9UniversitetskayaEmb., St. Petersburg, 199034, Russia
Koshlan.tetiana@gmail.com
ORCID: 0000-0002-0238-2909

СВЕДЕНИЯ ОБ АВТОРАХ

ГОЛОВИЦКИЙ Александр Петрович – *доктор физико-математических наук, профессор Высшей инженерно-физической школы Санкт-Петербургского политехнического университета Петра Великого,* Санкт-Петербург, Россия.
195251, Россия, г. Санкт-Петербург, Политехническая ул., 29
alexandergolovitski@yahoo.com
ORCID: 0000-0003-4292-0959

КОНЦЕВАЯ Вера Геннадьевна – *старший преподаватель кафедры математики и теории игр Псковского государственного университета, г. Псков, инженер Высшей инженерно-физической школы Санкт-Петербургского политехнического университета Петра Великого,* Санкт-Петербург, Россия.
180000, Россия, г. Псков, пл. Ленина, 2
nkoncevoi@mail.ru
ORCID: 0000-0002-1434-5056

КУЛИКОВ Кирилл Геннадьевич – *доктор физико-математических наук, профессор Высшей школы биомедицинских технологий Санкт-Петербургского политехнического университета Петра Великого,* Санкт-Петербург, Россия.
195251, Россия, г. Санкт-Петербург, Политехническая ул., 29
kulikov.kirill.g@gmail.com
ORCID: 0000-0002-4610-7394

КОШЛАН Татьяна Викторовна – *кандидат физико-математических наук, научный сотрудник Санкт-Петербургского государственного университета, Санкт-Петербург, Россия.*
199034, Россия, Санкт-Петербург, Университетская наб., 7–9
Koshlan.tetiana@gmail.com
ORCID: 0000-0002-0238-2909

Received 12.09.2023. Approved after reviewing 05.10.2023. Accepted 05.10.2023.
Статья поступила в редакцию 12.09.2023. Одобрена после рецензирования 05.10.2023. Принята 05.10.2023.